Human CYP4F3s are the main catalysts in the oxidation of fatty acid epoxides

Valérie Le Quéré,* Emmanuelle Plée-Gautier,* Philippe Potin,† Stéphanie Madec,† and Jean-Pierre Salaün[1,†]

Laboratoire de Biochimie-Equipe d'Accueil 948,* Université de Bretagne Occidentale, Faculté de Médecine, CS 93837, 29238 Brest Cédex 3, France; and Unité Mixte de Recherche 7139 Centre National de la Recherche Scientifique/Goëmar/Université Pierre et Marie Curie,† Station Biologique, 29682 Roscoff, France

Abstract **CYP4F isoforms are involved in the oxidation of important cellular mediators such as leukotriene B_4 (LTB4) and prostaglandins. The proinflammatory agent LTB4 and cytotoxic leukotoxins have been associated with several inflammatory diseases. We present evidence that the hydroxylation of *Z*9(10)-epoxyoctadecanoic, *Z*9(10)-epoxyoctadec-*Z*12-enoic, and *Z*12(13)-epoxyoctadec-*Z*9-enoic acids and that of monoepoxides from arachidonic acid [epoxyeicosatrienoic acid (EET)] is important in the regulation of leukotoxin and EET activity. These three epoxidized derivatives from the C18 family (C18-epoxides) were converted to 18-hydroxy-C18-epoxides by human hepatic microsomes with apparent K_m values of between 27.6 and 175 μM. Among recombinant P450 enzymes, CYP4F2 and CYP4F3B catalyzed mainly the ω-hydroxylation of C18-epoxides with an apparent V_{max} of between 0.84 and 15.0 min^{-1}, whereas the apparent V_{max} displayed by CYP4F3A, the isoform found in leukocytes, ranged from 3.0 to 21.2 min^{-1}. The rate of ω-hydroxylation by CYP4A11 was experimentally found to be between 0.3 and 2.7 min^{-1}. CYP4F2 and CYP4F3 exhibited preferences for ω-hydroxylation of *Z*8(9)-EET, whereas human liver microsomes preferred *Z*11(12)-EET and, to a lesser extent, *Z*8(9)-EET. Moreover, vicinal diol from both C18-epoxides and EETs were ω-hydroxylated by liver microsomes and by CYP4F2 and CYP4F3. These data support the hypothesis that the human CYP4F subfamily is involved in the ω-hydroxylation of fatty acid epoxides. These findings demonstrate that another pathway besides conversion to vicinal diol or chain shortening by β-oxidation exists for fatty acid epoxide inactivation.**—Le Quéré, V., E. Plée-Gautier, P. Potin, S. Madec, and J-P. Salaün. **Human CYP4F3s are the main catalysts in the oxidation of fatty acid epoxides. *J. Lipid Res.* 2004.** 45: **1446–1458.**

Supplementary key words leukotoxin • epoxyeicosatrienoic acid • cytochrome P450 • oxylipin • liver • microsomes • recombinant cytochrome P450 • hydroxylation

Manuscript received 5 November 2003 and in revised form 8 April 2004.

Published, JLR Papers in Press, May 16, 2004.
DOI 10.1194/jlr.M300463-JLR200

In contrast to the extensive knowledge of the functional properties of the cytochrome P450-derived eicosanoids in human and rodents, the metabolism of octadecanoids is poorly known. Epoxidized fatty acids from the C18 family (C18-epoxides) such as *Z*9(10)-epoxyoctadecanoic acid [*Z*9(10)-EpSTA], *Z*9(10)-epoxyoctadec-*Z*12-enoic acid [*Z*9(10)-EpOME, leukotoxin], and *Z*12(13)-epoxyoctadec-*Z*9-enoic acid [*Z*12(13)-EpOME, isoleukotoxin] should be regarded as toxic and/or defensive substances in living beings because they have been described as toxic metabolites in mammals (1) and as defense compounds in infected plants (2, 3). The conversion of fatty acid epoxides to the corresponding vicinal diol by epoxide hydrolases (EHs) is thought to be the general pathway for fatty acid epoxide clearance (4–9), although recently, Fang et al. (10) reported the conversion of epoxyeicosatrienoic acid (EET) to a chain-shortened epoxide. *Z*9,10-Epoxystearic acid and leukotoxins, which are commonly found in tissues, are products of cytochrome P450 epoxygenases, mainly the CYP2 gene family (11, 12). Cytochrome P450 epoxygenases are predominantly expressed in liver but are also present in several organs, including the kidney

Abbreviations: AA, arachidonic acid; BSTFA, *N,O*-bistrimethylsilyltrifluoroacetamide; C18-epoxides, epoxidized derivatives from the C18 family; DHET, dihydroxyeicosatrienoic acid; DiOME, dihydroxyC18:1 acid (vicinal diol); DiSTA, dihydroxystearic acid (vicinal diol); EET, epoxyeicosatrienoic acid; EH, epoxide hydrolase; HEET, hydroxyepoxyeicosatrienoic acid; HEpOME, hydroxyepoxyoctadecanoic acid; HEpSTA, hydroxy-9(10)-epoxyoctadecanoic acid; HETE, hydroxyeicosatetraenoic acid; LC-MS, liquid chromatography-mass spectrometry; LTB4, leukotriene B_4; Me/TMS, methyl ester trimethylsilyl ether; PPARα, peroxisome proliferator-activated receptor α; RP, reversed-phase; Rt, retention time; TMCS, trimethylchlorosilane; TriHET, trihydroxyeicosatrienoic acid; TriSTA, trihydroxystearic acid (triol); *Z*9(10)-EpOME, *Z*9(10)-epoxyoctadec-*Z*12-enoic acid; *Z*12(13)-EpOME, *Z*12(13)-epoxyoctadec-*Z*9-enoic acid; *Z*9(10)-EpSTA, *Z*9(10)-epoxyoctadecanoic acid (epoxystearic acid).

[1] To whom correspondence should be addressed.
e-mail: jp.salaun@univ-brest.fr

The online version of this article (available at http://www.jlr.org) contains an additional four tables and six figures.

(1). Leukotoxin and isoleukotoxin were shown to be generated by cells from the immune system (13) and by human liver (1, 14), but it is likely that several other P450 epoxygenase-containing tissues produce them. Furthermore, leukotoxin and isoleukotoxin are released from phospholipid epoxide by phospholipase A_2 (15) and are possibly produced by activated oxygen species generated during an oxidative burst. They are also associated with acute respiratory distress syndrome and severe burns (16). In addition, they are found in many polymeric plant cuticles as constitutive monomers (17) and hence can be derived from vegetable food intake. The biological roles of these products and derivatives are still poorly understood. However, monoepoxides of linoleic acid are known to cause disruption of mitochondrial function before cell death at pathologically relevant concentrations (1); they also induce chemotaxis in human neutrophils (18) and are associated with several inflammatory diseases. Leukotoxins as well as other epoxides of unsaturated fatty acids have been identified in infracted tissue, in which their amounts increased over time during ischemia compared with the surrounding healthy heart tissue (19).

One the other hand, arachidonic acid (AA) can be metabolized by cytochrome P450 enzymes to many biologically active compounds, including *Z*5(6)-, *Z*8(9)-, *Z*11(12)-, and *Z*14(15)-EETs, their corresponding dihydroxyeicosatrienoic acids (DHETs) (10), and 19- and 20-hydroxyeicosatetraenoic acids (HETEs). EETs are products of cytochrome P450 epoxygenase, mainly CYP2C8 in human liver (20, 21); they are endowed with important vasodilatating and antiinflammatory properties and serve as components of cell signaling cascades (22–26). EETs were shown to accumulate in alcoholic liver disease in rat (27) and increased in the rat kidney during liver cirrhosis (28). Cytochrome P450 monooxygenases are involved in both the epoxidation and hydroxylation of fatty acids (FAs). However, because of the remarkable diversity of P450 enzymes, it is difficult to pinpoint exactly which isoform is responsible for the regioselective oxidation of a fatty acid. ω-Hydroxylation of FAs is mainly catalyzed by the CYP4 family. Induction of members of the CYP4 family is thought to be associated with detoxification and secondary messenger production; the former is needed to maintain membrane integrity, and the messengers produced mediate many cellular processes and important physiological functions (29). The human CYP4F subfamily contains six members denoted F2, F3A, F3B, F8, F11, and F12. The closely homologous CYP4F2 and CYP4F3 (30, 31) from human liver (CYP4F3B) and polymorphonuclear leukocytes (CYP4F3A) were found to metabolize leukotriene B_4 (LTB4) to 20-hydroxy-LTB4. LTB4 is a potent lipid mediator involved in host defense and inflammatory responses. ω-Oxidation of leukotrienes is a major pathway in the degradation and inactivation of these proinflammatory mediators. CYP4F2 is catalytically distinct from CYP4F3 because of its inability to ω-hydroxylate lipoxin B (4). Furthermore, according to a recent report, CYP4F2 is the principal catalyst of vitamin E oxidation (32). Very recently, functionally distinct CYP4F3 isoforms showing tissue-specific expression patterns have been characterized in human. CYP4F3B is expressed in fetal and adult livers but not in neutrophils, although they express the CYP4F3A isoform (33). CYP4F2 expression has been detected in hepatic carcinoma, and high levels have been reported in the skin, followed by the kidney, prostate, liver, intestine, and brain (34, 35). CYP4F2 is constitutively expressed in a human hepatoma cell line, HepG2, and is not induced by clofibrate (36). On the other hand, a very recent study (22) has challenged the view that ω-hydroxylation of EETs is a degradation pathway of EETs and suggests that this process is involved in the biogenesis of secondary messengers capable of binding to the nuclear hormone receptor peroxisome proliferator-activated receptor α (PPARα) with high affinity. The authors of that report also indicate that ω-hydroxyepoxyeicosatetraenoic acid (ω-HEET) are generated by the CYP4A family from rat liver and suggest that ω-HEETs are the endogenous ligands of this nuclear receptor involved in lipid homeostasis.

Elucidation of the pathway that synthesizes epoxides from unsaturated C18 fatty acids and AA in hepatic human microsomes might provide important clues to the roles of epoxides in various physiological processes. The purpose of the present study was to delineate and to tentatively characterize the human cytochrome P450 enzymes involved in these oxidation reactions. We investigated the metabolism of three epoxides derived from unsaturated fatty acids of the C18 family and of four isomeric EETs using both human microsomes and a series of human recombinant cytochrome P450s.

MATERIALS AND METHODS

Chemicals

Radiolabeled [1-^{14}C]lauric acid (45 Ci/mol), [1-^{14}C]oleic acid (50 Ci/mol), and [1-^{14}C]linoleic acid (58 Ci/mol) were from Amersham. [1-^{14}C]*Z*9(10)-EpSTA (5.7 Ci/mol), [1-^{14}C]*Z*9(10)-EpOME (6.4 Ci/mol), and [1-^{14}C]*Z*12(13)-EpOME (6.2 Ci/mol) were from Commissariat à l'Energie Atomique (Gif sur Yvette, France). AA, *Z*5(6)EET, *Z*8(9)EET, *Z*11(12)EET, *Z*14(15)EET, *Z*9(10)-EpSTA, *Z*9(10)-EpOME, *Z*12(13)-EpOME, palmitoleic acid, lauric acid, and α-tocopherol were obtained from Cayman Chemicals (SPI Bio, Massy, France). NADPH was purchased from Sigma Chimie (La Verpillière, France). The silylating reagent used, *N,O*-bistrimethylsilyltrifluoroacetamide (BSTFA), contained 1% trimethylchlorosilane (TMCS) and was from Pierce Europe (Oud-Beijerland, The Netherlands). 3-Chloroperoxybenzoic acid was from Fluka (S'Quentin Fallavier, France). The modified, human P450-containing cell microsomes (Supersomes™) were obtained from Gentest (Woburn, MA), whereas cytochrome b_5 was from Oxford Biomedical Research (Oxford, MI). Cytochrome P450 from control Supersomes™ was not detectable. All chemicals and solvents were from Merck (Darmstadt, Germany) and Sigma.

Synthesis of radiolabeled epoxides and 9,10-dihydroxystearic acid

[1-^{14}C]*Z*9(10)-epoxystearic acid and [1-^{14}C]leukotoxins [*Z*9(10)-EpOME and *Z*12(13)-EpOME] were synthesized from [1-^{14}C]oleic acid (specific activity of 60 Ci/mol) and [1-^{14}C]

linoleic acid (specific activity of 55 Ci/mol), respectively. The epoxidation of each substrate was performed in a reaction mixture (0.2 ml) containing either 0.35 mM epoxystearic acid or 0.33 mM leukotoxins together with 1.8 mM 3-chloropreoxybenzoic acid. The reaction was initiated for 5 min at ambient temperature by the addition of 3-chloroperoxybenzoic acid and terminated by evaporation under N_2. The C18-epoxides [*Z*9(10)-EpSTA, *Z*9(10)-EpOME, and *Z*12(13)-EpOME] were purified by reverse phase (RP)-HPLC, collected, and extracted twice with diethyl ether. Then, the organic phase was evaporated and radiolabeled compounds (~98% pure) were dissolved in ethanol. Radiolabeled epoxides were isotopically diluted to have a final specific activity of 13.3 Ci/mol in 0.2 ml of reaction mixture.

For the synthesis of 9,10-dihydroxystearic acid (9,10-DiSTA), *Z*9(10)-EpSTA was treated with 20% NaOH for 1 h at room temperature. Then, this mixture was acidified with chlorhydric acid (1 N), extracted with diethyl ether, and analyzed by RP-HPLC. The collected vicinal diol was ~98% pure.

Human recombinant P450s and liver microsomes

Human liver samples were obtained from 16 Caucasian multiorgan donors (9 males and 7 females; mean ± SD age of 40 ± 15 years) who had died after traffic accidents or disease. Ethical committee approval was obtained before studies in accordance with French law. Microsomes from seven human livers (subject BR) were prepared after homogenization of the tissues as previously described (37) and stored at −80°C until use. Samples from other subjects were from Gentest (subject H and HG). Most of the studies were performed with liver microsomes from subject BR065. The presence of a microsome-associated epoxide hydrolysis (EH)-like activity in the Supersomes™ preparations enabled us to highlight the formation of trihydroxy released by the hydrolysis of the oxirane from epoxydated ω-hydroxy or by ω-hydroxylation of the vicinal diol derivatives. Depending on whether the membrane preparation contained or did not contain recombinant P450, EH-like activity was between 0.15 and 0.55 nmol/min/mg protein.

Microsomal protein concentrations were determined using the Bradford method (Bio-Rad, Munich, Germany). Cytochrome P450 content was measured by spectrophotometry according to Omura and Sato (38).

Fatty acid oxidation assays

Microsomes containing the human cytochromes P450 reductase and cytochrome b_5 (Supersomes™) were prepared from baculovirus-infected BTI-TH-5B1-4 cells provided by Gentest. The specific contents of CYP samples were as follows: CYP2C8, 244 pmol/mg protein; CYP2C9, 357 pmol/mg protein; CYP2E1, 444 pmol/mg protein; CYP3A4, 127 pmol/mg protein; CYP4A11, 111 pmol/mg protein; CYP4F2, 556 pmol/mg protein; CYP4F3A, 36 pmol/mg protein, and CYP4F3B, 333 pmol/mg protein. Control Supersomes™ CYP450 content was not detectable.

All monooxygenase activities, except for the metabolism of EET, were measured by using radiolabeled 1-^{14}C-substrates. After isotopic dilution with unlabeled material, the substrates (specific activity of 0.5 Ci/mol) were dissolved in ethanol. Routinely, substrate conversion to oxidized metabolites was determined in a reaction mixture (0.2 ml) containing 75 μM ethanol-free substrate, 0.3 mg of microsomal protein or Supersomes™ (33 pmol of CYP4F3B, 56 pmol of CYP4F2, 7 pmol of CYP4F3A, 22 pmol of CYP4A11, 25 pmol of CYP3A4, 89 pmol of CYP2E1, 79 pmol of CYP2C8, and 71 pmol of CYP2C9), 0.1 M sodium phosphate buffer (pH 7.4), and 1 mM NADPH. The reaction was initiated by the addition of NADPH and then terminated after 10 min (except otherwise noted) at 37°C with a volume of 200 μl of acetonitrile containing 0.2% acetic acid. Metabolites and residual substrates were extracted twice with 5 ml of ethyl acetate. The organic phase was dried under a stream of nitrogen, and the residue was dissolved in methanol before RP-HPLC analysis. The product and residual substrate were detected by radioactivity using a β-radiometric HPLC detector (Flo-one Beta Radiometric Detector; Packard) or by mass spectrometry {atmospheric pressure chemical ionization on negative mode [APCI$^{(-)}$]} coupled to RP-HPLC. The enzyme activity was measured with a limit of detection of ~0.009 nmol/min when liquid chromatography-mass spectrometry (LC-MS) was used to quantify the reaction products. Each assay was performed in triplicate. Metabolites were further characterized by GC-MS. For kinetic studies in human liver microsomes, the parameters of apparent K_m and V_{max} were determined from subject BR065 and calculated using Sigma Plot 8.0 software. The kinetic experiments were carried out with substrate at five different concentrations between 10 and 100 μM, except as noted. Note that the kinetic values of enzymes were probably underestimated in this study because of *i*) the presence in membrane preparations from human microsomes and insect cells expressing recombinant P450s of a second enzyme (EH-like) mediating the conversion of epoxide to vicinal diol and competing with cytochrome P450s for the substrate, and *ii*) the competition between the epoxide and the vicinal diol for ω-hydroxylation by P450s.

RP-HPLC analysis of metabolites

The oxidized metabolites and residual substrate were separated by RP-HPLC using a 5 μm Ultrasphere C18 column (150 × 4.6 mm; Beckman). The mobile phase consisted of a mixture of water and acetonitrile (with 0.2% acetic acid) (65:35, v/v) for both epoxystearic acid and leukotoxins at a flow rate of 2 ml/min. Isocratic elution was carried out for 35 min. Then, each of the residual substrates was eluted by applying a mixture of water-acetonitrile (5:95, v/v) containing 0.2% acetic acid for 10 min before returning to the initial conditions. The radioactivity of RP-HPLC effluent was monitored with a computerized online scintillation counter (Flo-one Beta Radiometric Detector). The rate of generated radiolabeled metabolites was calculated from peak areas.

Chiral analysis

Chiral analysis was performed as previously described (39) using optically pure synthetic 9*R*,10*S*-epoxystearate methyl ester as a standard. Briefly, radiolabeled enantiomers of epoxystearic acid were separated by HPLC (Spectra System P400 with ultraviolet detector UV1000) using a chiral column [Column Chiracel OB (4.6 × 250 mm); J.J. Baker Chemical Co.]. Enantiomers of 18-hydroxy-C18-epoxides were analyzed as methyl ester derivatives and resolved using a mixture of solvents (hexane-isopropanol-acetic acid, 90:10:0.1, v/v/v) in isocratic mode for 60 min; for residual C18-epoxides, the solvent mixture was hexane-isopropanol-acetic acid (99.7:0.2:0.1, v/v/v) at a flow of 0.8 ml/min. Radioactivity of the HPLC effluent was monitored with a computerized online liquid scintillation counter (Flo-one Beta Radiometric Detector).

LC-MS analysis

Oxidized metabolites were separated by LC using an Ultrasphere C18 column (250 × 4.6 mm; Beckman) and identified by mass spectrometry. The mass spectrometer (Navigator; Finnigan) was equipped with an ionization source at atmospheric pressure (APCI$^-$) running in negative ion mode (cone voltage of 30–45 V) and operated in full-scan MS mode. The same mobile phase described above for RP-HPLC analysis was used at a flow

rate of 1 ml/min. A 30 min isocratic elution with water-acetonitrile (40:60, v/v) containing 0.2% acetic acid allowed the separation of metabolites. This was followed with a 10 min linear gradient of water-acetonitrile (5:95, v/v) with 0.2% acetic acid to elute the substrates. For analysis by mass spectrometry, negative ions were monitored by full scan from *m/z* 60 to 600. The source heater and the APCI$^-$ heater were at 150°C and 350°C, respectively, with a cone voltage of either 30 or 45 V to increase fragmentation. Detection of metabolites was achieved by monitoring selected ions corresponding to the expected carboxylate anions [M-H]$^-$. Compounds were quantified by LC-MS from standard curves obtained by measuring peak surfaces of authentic compounds when available from at least five concentrations.

GC-MS analysis

GC-MS analysis was carried out on a gas chromatograph (HP 5890 Series II gas chromatograph; Agilent Technology) equipped with a fused silica capillary column (HP-5MS 5% phenyl methyl siloxane; 30 m × 0.32 mm inner diameter, 0.25 μm thick film). The gas chromatograph was combined with a quadrupole mass-selective detector (HP 5971A; Agilent Technology). Mass spectra were recorded at 70 eV in the electron impact mode.

Analysis was performed after methylation with etheral diazomethane and silylation with 100 μl of a mixture of BSTFA/TMCS (1%) for 60 min at 60°C to obtain methyl ester trimethylsilyl ether (Me/TMS) derivatives. Compounds were dissolved in 90 μl of hexane, and 2 μl was injected in the splitless mode at 250°C. After 5 min at 60°C, the oven temperature was increased to 200°C at 50°C/min and then linearly ramped to 280°C at 2°C/min to let it stabilize for 10 min before coming back to the initial conditions.

Mass spectra of Me/TMS derivatives showed typical fragment ions at *m/z* = 73 (TMS), [M-15]$^+$, [M-31]$^+$, [M-47]$^+$. The most characteristic fragment ions used to determine the structures of positional isomers generated are given in Tables I and II (see supplemental data).

RESULTS

Metabolism of fatty acid epoxides

To assess whether cytochrome P450 enzymes are involved in the metabolism of fatty acid epoxides from both C18 (**Fig. 1**) and AA, we first examined this reaction in hepatic microsomes from human. After the addition of NADPH, liver microsomes converted *Z*9(10)-EpSTA, *Z*9(10)-EpOME, and *Z*12(13)-EpOME as well as the four AA monoepoxides mainly to ω-hydroxy derivatives (Fig. 1) in a time-dependent manner (data not shown). A representative elution profile of metabolites generated from *Z*9(10)-EpSTA by RP-HPLC with radioactivity detection is given in **Fig. 2**. Similar profiles were obtained for *Z*9(10)-EpOME, *Z*12(13)-EpOME, and EETs. The RP-HPLC and GC retention times (Rts) of metabolites are given in Tables I and II (see supplemental data). As expected for P450 reaction, these ω-hydroxylations were NADPH dependent but CO inhibited. In the absence of NADPH, only one metabolite was generated via an EH-like enzyme

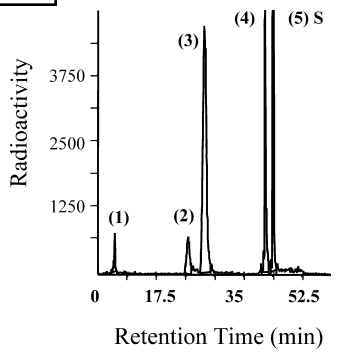

Fig. 2. Representative reversed-phase (RP)-HPLC analysis of the metabolites generated by human liver microsomes incubated with *Z*9(10)-EpSTA using radioactivity detection. Liver microsomes (0.3 mg protein) were incubated with [1-^{14}C]*Z*9(10)-EpSTA (75 μM) in the presence of NADPH. After 10 min at 37°C, the organic soluble products were extracted, resolved, and quantified as described in Materials and Methods. All peaks were collected for further identification by GC-MS. Peak 1, mixture of 9,10,18-trihydroxyoctadecanoic and 9,10,17-trihydroxyoctadecanoic acids; peak 2, 17-hydroxy-9(10)-epoxyoctadecanoic acid [ω-1; 17,9(10)-HEpSTA]; peak 3, 18-hydroxy-9(10)-epoxyoctadecanoic acid [ω; 18,9(10)-HEpSTA]; peak 4, 9,10-dihydroxyoctadecanoic acid; peak 5, residual substrate (S).

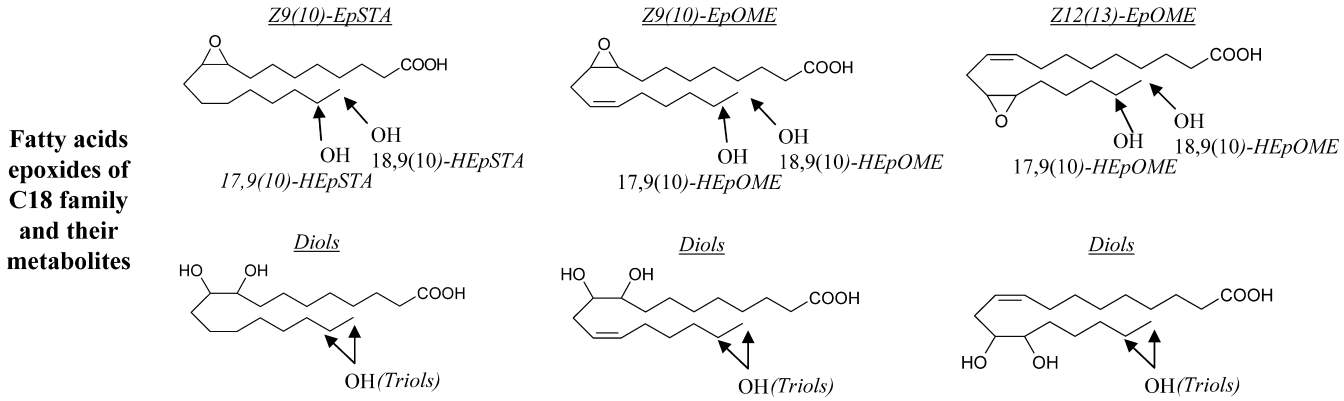

Fig. 1. Chemical structures of fatty acid epoxides and derivatives from the C18 family. Metabolism of epoxides results in the formation of several similar hydroxylated metabolites (ω-OH, vicinal diol, and triol). EpOME, epoxyoctadecanoic acid; EpSTA, epoxyoctadecanoic acid; HEpOME, hydroxyepoxyoctadecanoic acid; HEpSTA, hydroxyepoxyoctadecanoic acid.

leading to the corresponding vicinal diol. Less than 5% of the initial substrate was converted to uncharacterized metabolites by incubating *Z*9(10)-epoxystearic acid with buffer alone, heat-killed human microsomes, and recombinant P450s for 45 min at room temperature. Metabolites were structurally characterized by APCI$^-$-LC-MS and GC-MS as Me/TMS derivatives (see supplemental data). The ratios of ω-/(ω-1)-hydroxylated metabolites were very similar for *Z*9(10)-EpSTA and *Z*9(10)-EpOME (~8.2 and 6.9, respectively) but decreased to 1.6 for *Z*12(13)-EpOME hydroxylation.

To decipher the major pathways of hydroxylation in hepatic human microsomes, we further investigated the metabolism of each class of FA epoxides.

Metabolism of 9,10-epoxystearic acid by liver microsomes from human

The kinetic parameters of the hydroxylation reactions of FA epoxides were mainly determined using liver microsomes from subject BR065. The metabolism of *Z*9(10)-EpSTA was investigated with human liver microsomes. Four metabolites were generated from [1-^{14}C]*Z*9(10)-EpSTA by the microsomal fraction in the presence of NADPH. A representative profile of LC-MS analysis (APCI$^-$) of metabolites generated from *Z*9(10)-EpSTA by these human microsomes is given on **Fig. 3**. When NADPH was missing, only one metabolite (Fig. 3, peak 4) was generated through the action of an EH-like activity, and this led to the synthesis of the corresponding vicinal diol, 9,10-DiSTA. Selective ion monitoring showed the presence of negative ions $(M\text{-}H)^-$ at *m/z* 331 in peak 1 (Rt, 3.7 min) corresponding to a mixture of 9,10,17- and 9,10,18-trihydroxyC18:0 [9,10,17-trihydroxystearic acid (TriSTA) and 9,10,18-TriSTA]; at *m/z* 313 in peaks 2 and 3 (Rt, 8.0 and 8.8 min) corresponding to 17-hydroxy- and 18-hydroxy-9(10)-epoxystearic acid [17,9(10)-HEpSTA and 18,9(10)-HEpSTA], respectively; at *m/z* 315 in peak 4 (Rt, 18.5 min) corresponding to 9,10-DiSTA (vicinal diol); and at *m/z* 297 in peak 5 (Rt, 46.0 min) corresponding to the residual substrate. Hydroxylation of the vicinal diol to 9,10,18-TriSTA was confirmed by incubating 9,10-DiSTA, obtained by chemical hydrolysis of *Z*9(10)-epoxystearic acid (see Materials and Methods), with microsomes. Our results show that both human microsomes and CYP4F3 (A and B) are able to convert 9,10-DiSTA (75 μM) to 9,10,18-TriSTA with a velocity of 0.115 nmol/min/mg protein, 10.1 nmol/min/nmol P450 (CYP4F3A), and 10.5 nmol/min/nmol P450 (CYP4F3B), respectively. APCI$^-$ analysis of 18,9(10)-HEpSTA and 17,9(10)-HEpSTA yielded mass spectra with informative and characteristic ions, as shown in **Fig. 4**. Analysis of the metabolites (Me/TMS derivatives) by GC-MS confirms these chemical structures (Fig. I, see supplemental data). Informative and selective ion fragments of each compound are given in Table I (see supplemental data). These results indicate that in addition to being converted to vicinal diol by EH-like, *Z*9(10)-EpSTA can undergo ω- and (ω-1)-hydroxylation and that the vicinal diols are themselves converted to the 9,10,18-TriSTA (Fig. 2, peak 1). Apparent kinetic constants for the oxidation of *Z*9(10)-EpSTA to hydroxylated metabolites by the microsomal preparation were estimated from detailed investigations of epoxide hydroxylation at various substrate concentrations. The liver microsomes converted *Z*9(10)-EpSTA to 18,9(10)-HEpSTA with an apparent K_m of 27.6 μM and an apparent V_{max} of 2.5 nmol/min/mg protein (3.7 nmol/min/nmol P450) and to 17,9(10)-HEpSTA with an apparent K_m of 27.9 μM and an apparent V_{max} of 0.45 nmol/min/mg protein (0.66 nmol/min/nmol P450) using a substrate concentration range of 10–100 μM (**Table 1**). As a comparison, the apparent K_m of human liver microsomes for the conversion of LTB4 to 20-hydroxy-LTB4 was determined to be 74.8 μM with a V_{max} of 2.42 nmol/min/nmol P450 (40). Interindividual variation in the initial rate of oxidation of *Z*9(10)-EpSTA was

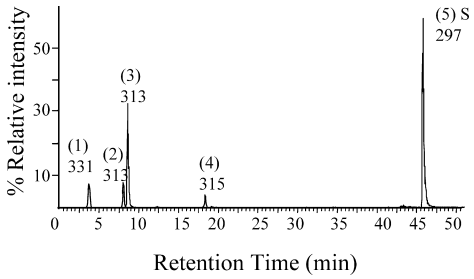

Fig. 3. Representative RP-HPLC analysis of the metabolites generated by human liver microsomes incubated with *Z*9(10)-EpSTA using mass spectrometric detection. Liver microsomes (0.3 mg protein) were incubated with *Z*9(10)-EpSTA (75 μM) in the presence of NADPH. After 10 min at 37°C, the organic soluble products were extracted, resolved, and detected by monitoring selected ions corresponding to the expected carboxylate anions $[M\text{-}H]^-$ as described in Materials and Methods. Peak 1, mixture of 9,10,18-trihydroxyoctadecanoic and 9,10,17-trihydroxyoctadecanoic acids, *m/z* = 331; peak 2, 17,9(10)-HEpSTA [(ω-1)-OH], *m/z* = 313; peak 3, 18,9(10)-HEpSTA (ω-OH), *m/z* = 313; peak 4, 9,10-dihydroxyoctadecanoic acid, *m/z* = 315; peak 5, residual substrate (S).

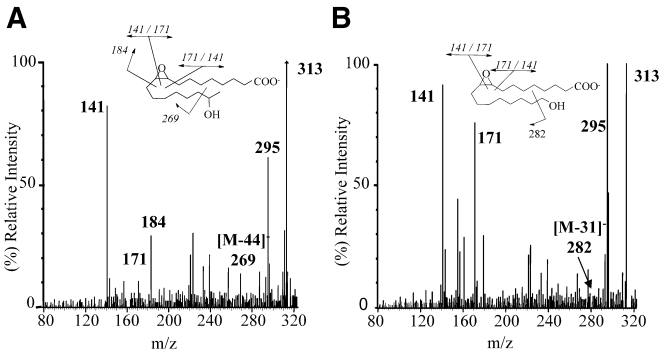

Fig. 4. LC-MS mass spectra of hydroxylated derivatives of *Z*9(10)-EpSTA generated by human liver microsomes. A: 17,9(10)-HEpSTA. B: 18,9(10)-HEpSTA. *Z*9(10)-EpSTA (75 μM) was incubated with 0.3 mg of human liver microsomes and 1 mM NADPH at 37°C for 10 min. Metabolites were analyzed by RP-HPLC with mass spectrometric detection (APCI$^-$) as described in Materials and Methods.

TABLE 1. Kinetic parameters of ω- and (ω-1)-hydroxylated derivatives of C18-epoxides in human liver microsomal preparations

Human Liver (BR065)	(ω-1)-Hydroxylation		ω-Hydroxylation	
	K_m	V_{max}	K_m	V_{max}
	μM	*nmol/min/mg prot.*	*μM*	*nmol/min/mg prot.*
Z9(10)-EpSTA	27.9	0.45	27.6	2.5
Z9(10)-EpOME	51.2	0.26	175	2.3
Z12(13)-EpOME	15.4	0.11	27.6	0.81

C18-epoxide, epoxidized derivative from the C18 family; Z9(10)-EpOME, Z9(10)-epoxyoctadec-12-enoic acid; Z12(13)-EpOME, Z12(13)-epoxyoctadec-9-enoic acid; Z9(10)-EpSTA, Z9(10)-epoxyoctadecanoic acid. Samples containing 0.3 mg of protein (0.68 nmol of P450 per milligram of protein) were incubated at 37°C for 10 min with increasing concentrations of C18-epoxide ranging from 10 to 100 μM and analyzed by reversed-phase (RP)-HPLC with radiometric detection as described in Materials and Methods. Values shown are averages of triplicate determinations that differ for less than 10% of the mean.

determined using 16 samples of liver microsomes from Caucasian adult subjects (**Table 2**). These experiments revealed a 3.1- and 4.2-fold variation in ω- and (ω-1)-hydroxylation activities [range, 0.56–1.72 nmol/min/mg protein for ω-hydroxylation and 0.09–0.38 for (ω-1)-hydroxylation], respectively. The cytochrome P450 content was in the range of 0.25–0.68 pmol/mg protein (2.7-fold variation). Among the 16 human liver samples we tested, 3.1- and 34.5-fold variations were noted in the formation of

TABLE 2. Metabolism of Z9(10)-EpSTA by human liver microsomes from 16 individual Caucasian subjects

Subject	P450 Content	Enzyme Activities			
		TriSTA	(ω-1)-OH	ω-OH	DiSTA
	nmol/mg protein	*nmol/min/mg protein*			
BR062	0.67	0.50	0.17	0.95	0.41
BR063	0.52	0.61	0.38	1.44	0.24
BR065	0.68	0.69	0.38	1.69	0.30
BR016	0.37	0.08	0.14	1.27	0.29
BR035	0.25	0.07	0.22	1.05	0.39
BR034	0.29	0.11	0.24	1.72	0.42
BR018	0.33	0.02	0.10	0.78	0.34
HK27	0.30	0.11	0.09	0.64	0.69
HK23	0.38	0.07	0.11	0.67	0.68
HK31	0.58	0.19	0.10	0.56	0.69
HG56	0.55	0.20	0.12	0.79	0.55
HG43	0.26	0.29	0.09	0.70	0.75
HG42	0.67	0.19	0.12	0.71	0.66
HG6	0.30	0.24	0.09	0.68	0.65
HG3	0.29	0.14	0.09	0.87	0.44
HG88	0.39	0.18	0.11	0.87	0.53

Z9(10)-EpSTA (75 μM) was incubated with 0.3 mg of microsomal protein and 1 mM NADPH at 37°C for 10 min. Values shown are averages of triplicate determinations that differ for less than 15% of the means. The metabolites 17-hydroxy-9(10)-epoxyoctadecanoic acid [17,9(10)-HEpSTA; (ω-1)-OH], 17-hydroxy-9(10)-epoxyoctadecanoic acid [18,9(10)-HEpSTA; (ω-OH)], dihydroxylated derivatives [dihydroxystearic acid (DiSTA)], and trihydroxylated derivatives, as a mixture of ω- and (ω-1)-hydroxylated DiSTA [trihydroxystearic acid (TriSTA)], were separated and quantified by RP-HPLC with radiometric detection, and P450 content was measured as described in Materials and Methods.

TABLE 3. Metabolism of Z9(10)-EpSTA with genetically engineered human P450 isoforms

Recombinant P450	Enzyme Activities			
	TriSTA	(ω-1)-OH	ω-OH	DiSTA
	nmol/min/nmol P450			*nmol/min/mg protein*
CYP4A11	0	0.58	2.7	0.04
CYP2E1	0	0	0	0.09
CYP2C8	0	0.31	0	0.08
CYP2C9	0	0.49	0.29	0.10
CYP3A4	0	0.58	0.52	0.18
CYP4F3B	0.16	0.53	12	0.14
CYP4F3A	0	0	11	0.14
CYP4F2	0.21	0.25	5	0.55

Z9(10)-EpSTA (75 μM) was incubated with recombinant proteins and 1 mM NADPH at 37°C for 40 min. Values shown are averages of triplicate determinations that differ for less than 10% of the means. The metabolites 17,9(10)-HEpSTA [(ω-1)-OH], 18,9(10)-HEpSTA (ω-OH), dihydroxylated derivatives (DiSTA), and trihydroxylated derivatives, as a mixture of ω- and (ω-1)-hydroxylated DiSTA (TriSTA), were separated and quantified by RP-HPLC with radiometric detection as described in Materials and Methods.

vicinal diol and triol (respective ranges, 0.24–0.75 and 0.02–0.69 nmol/min/mg protein).

Metabolism of 9,10-epoxystearic acid by recombinant P450 from human

The results of incubation of Z9(10)-EpSTA with a series of recombinant human P450s expressed in insect cells (Supersomes™) are shown in **Table 3**. Of eight recombinant P450 isoforms tested, only human CYP4F2, CYP4F3, and CYP4A11 were capable of significantly catalyzing the hydroxylation of Z9(10)-EpSTA (75 μM). CYP4F2 and CYP4F3B were also capable of catalyzing mainly the ω-hydroxylation of the vicinal diol, generated by EH-like activity, into 9,10,18-TriSTA (Table 3).

The highest turnover rate for the ω-hydroxylation of Z9(10)-EpSTA was measured for CYP4F3B (12 min^{-1}), followed by CYP4F3A (11 min^{-1}), CYP4F2 (5 min^{-1}), and CYP4A11 (2.7 min^{-1}). Apart from CYP4F3A, the three other isoforms catalyzed the (ω-1)-hydroxylation leading to the formation of 17,9(10)-HEpSTA with a turnover rate ranging from 0.25 to 0.58 min^{-1}. However, CYP2C8, CYP2C9, and CYP3A4 were found to mainly generate 17,9(10)-HEpSTA with a turnover rate ranging from 0.31 to 0.58 min^{-1}, although no activity was detected for CYP2E1. Analysis of the 18-hydroxylation of Z9(10)-EpSTA by CYP4F2 and CYP4F3 in a representative experiment revealed kinetic parameters with an apparent K_m ranging from 6.3 to 35.7 μM and an apparent V_{max} ranging from 7.9 to 13.2 nmol/min/nmol P450. CYP4F3A had a V_{max}/K_m value of 1.7 for Z9(10)-EpSTA, which is ~5-fold higher than that for CYP4F3B and CYP4F2 (**Table 4**). The differences in catalytic activities between CYP4F3A and CYP4F3B appear less pronounced than has been reported (33) for LTB4 ω-hydroxylation by these P450 isoforms expressed in COS-7 cells. An apparent K_m of 4 μM was determined for CYP4F3A versus 105 μM for CYP4F3B (26-fold higher).

TABLE 4. Kinetic parameters of ω-hydroxylated derivatives of C18-epoxides by CYP4F isoforms

Isoform	Recombinant P450	ω-Hydroxylation K_m	ω-Hydroxylation V_{max}
		μM	*nmol/min/nmol P450*
*Z*9(10)-EpSTA	CYP4F3A	6.3	10.8
	CYP4F3B	35.7	13.2
	CYP4F2	26.1	7.9
*Z*9(10)-EpOME	CYP4F3A	46.6	21.2
	CYP4F3B	108.1	15.02
	CYP4F2	163.1	10.6
*Z*12(13)-EpOME	CYP4F3A	61.8	3
	CYP4F3B	100.6	3.93
	CYP4F2	135	0.84

Samples containing human recombinant CYP4F isoforms were incubated at 37°C for 40 min, with increasing concentrations of C18-epoxide ranging from 5 to 100 μM, and analyzed by RP-HPLC with radiometric detection as described in Materials and Methods. Values shown are averages of triplicate determinations that differ for less than 10% of the means.

Inhibition studies

Further screening showed that the ω-hydroxylation of *Z*9(10)-EpSTA was completely inhibited in human microsomes by LTB4, a substrate of CYP4F2, CYP4F3, and CYP4F12. On the other hand, lauric acid, a substrate of CYP4A11, but not of CYP4F, caused no inhibition. The data in **Table 5** clearly indicate that the presence of laurate (50 μM) in the incubation medium of human liver microsomes (subject BR065) had no effect on the rate of *Z*9(10)-EpSTA, *Z*9(10)-EpOME, and *Z*12(13)-EpOME hydroxylations. On the other hand, lauric acid strongly inhibited both the ω- and (ω-1)-hydroxylation of *Z*9(10)-EpSTA by CYP4A11 (97% and 77%, respectively), although CYP4F2 and CYP4F3B activities remained unaffected. Similar results were obtained with *Z*9(10)-EpOME and *Z*12(13)-EpOME as substrates (data not shown). We investigated the effects of 50 μM LTB4 on the hydroxylation of *Z*9(10)-EpSTA by liver microsomes and on that of three recombinant P450s from human liver. When LTB4 was present, only one metabolite, the vicinal diol issued from the oxirane hydrolysis of *Z*9(10)-EpSTA, was generated by the liver microsomal EH-like activity from at least three subjects (data not shown). Moreover, and as expected, oxidation of the substrate by CYP4F2 and CYP4F3B was inhibited by 98% and 100%, respectively. In a previous study (40), CYP4A11 isolated from human liver microsomes was shown to exhibit negligible LTB4 ω-hydroxylase activity. But in our investigations, the ω-hydroxylation of *Z*9(10)-EpSTA was totally inhibited when recombinant CYP4A11 was incubated in the presence of 50 μM LTB4. This last observation suggests the involvement of this isoform in LTB4 oxidation. This led us to reinvestigate the catalytic properties of CYP4A11 (Supersomes™) through the incubation of LTB4 as substrate. The generated metabolites (Me/TMS derivatives) were analyzed by GC-MS. The GC profile revealed the NADPH-dependent formation of a major metabolite at Rt

TABLE 5. Effects of lauric acid and LTB4 on the metabolism of radiolabeled *Z*9(10)-EpSTA, *Z*9(10)-EpOME, and *Z*12(13)-EpOME by human liver microsomes (subject BR065) and by recombinant P450 from human liver

Substrate (50 μM)	Recombinant P450 or Human Microsomes	Enzyme Activities: LTB4 (μM)	Triol	(ω-1)-OH	ω-OH	Diol
*Z*9(10)-EpSTA	Human liver microsomes	0	0.07	0.17	1.24	0.61
		50	0	0	0	1.08
	CYP4A11	0	0	0.57	3.90	0.16
		50	0	0	0	0.14
	CYP4F2	0	0	0.07	3.29	0.21
		50	0	0	0.07	0.20
	CYP4F3B	0	0.9	0.46	9.31	1.5
		50	0	0	0	1.5
		Lauric acid (μM)	Triol	(ω-1)-OH	ω-OH	Diol
*Z*9(10)-EpSTA	Human liver microsomes	0	0.047	0.12	0.98	0.43
		50	0.098	0.16	1.17	0.53
	CYP4A11	0	0.1	0.30	1.62	0.02
		50	0.028	0.07	0.05	0.11
	CYP4F2	0	0.45	1.32	4.38	0.14
		50	0.54	1.28	4.42	0.10
	CYP4F3B	0	0.05	0.23	2.64	0.07
		50	0.14	0.20	2.78	0.07
*Z*9(10)-EpOME	Human liver microsomes	0	0.40	0.14	0.96	1.03
		50	0.15	0.13	1.0	1.17
*Z*12(13)-EpOME	Human liver microsomes	0	0.52	0.21	0.34	0.20
		50	0.55	0.21	0.31	0.24

LTB4, leukotriene B_4. Membrane preparations from both liver microsomes and recombinant P450s were incubated (see Materials and Methods) with NADPH and radiolabeled FA epoxides (50 μM) in the presence or absence of lauric acid (50 μM) and LTB4 (50 μM) for 40 min. Values shown are averages of triplicate determinations that differ for less than 10% of the means and are expressed as nmol/min/nmol P450 for recombinant proteins and nmol/min/mg protein for activities of human microsomes. The hydroxylated products 17-hydroxyepoxide [(ω-1)-OH], 18-hydroxyepoxide (ω-OH), dihydroxylated derivatives (diol), and trihydroxylated derivatives, as a mixture of ω- and (ω-1)-hydroxylated diol (triol), were separated and quantified by RP-HPLC with radiometric detection as described in Materials and Methods.

37.1 min. Its mass spectrum was that expected for 20-hydroxy-LTB4 and very similar to a published spectrum with fragment ions at *m/z* 494, 479 [M^+-15], 463 [M^+-31]. The rate of formation of 20-hydroxy-LTB4 at a substrate concentration of 75 μM was measured in three independent incubations and found to be 1.8 nmol/min/nmol P450. All of these experimental data led us to select CYP4 isoforms as possibly closely related to FA epoxide metabolism.

Leukotoxin and isoleukotoxin metabolism by liver microsomes from human

Kinetic studies of the *Z*9(10)-EpOME and *Z*12(13)-EpOME hydroxylation reactions were carried out with liver microsomes from subject BR065. Across the range of substrate concentrations used (10–100 μM), the metabolism of *Z*9(10)-EpOME and *Z*12(13)-EpOME to the corresponding 18-hydroxylated derivatives seemed to follow simple Michaelis-Menten kinetics. Incubation of human liver microsomes (BR065) in the presence of NADPH with *Z*9(10)-EpOME and *Z*12(13)-EpOME generated four metabolites for both substrates. As for *Z*9(10)-EpSTA, in the absence of added NADPH substrates were converted to the corresponding vicinal diol. Table 1 gives the apparent kinetic parameters measured for the ω- and (ω-1)-hydroxylations of *Z*9(10)-EpOME and *Z*12(13)-EpOME. The apparent intrinsic clearance of liver (V_{max}/K_m ratio) for the ω-hydoxylation of *Z*9(10)-EpSTA was 7- and 3-fold that of *Z*9(10)-EpOME and *Z*12(13)-EpOME, respectively. The ratio of ω-/(ω-1)-hydroxylated metabolites was very similar for *Z*9(10)-EpSTA and *Z*9(10)-EpOME (~8.2 and 6.9, respectively) but decreased to 1.6 for *Z*12(13)-EpOME hydroxylation.

Metabolism of leukotoxin and isoleukotoxin by recombinant P450 from human

Simple Michaelis-Menten kinetic values were observed with recombinant CYP4F enzymes across the range of *Z*9(10)-EpOME and *Z*12(13)-EpOME concentrations used (10–100 μM). The values derived for CYP4F were almost of the same order of magnitude, with an apparent K_m of 46.6–163.1 μM and an apparent V_{max} in the range 0.84–21.2 min^{-1} (Table 4). Compared with the K_m values reported previously (41) for LTB4 ω-hydroxylation by CYP4F3A (0.68 μM) and CYP4F3B (20.6 μM), those we measured for ω-hydroxylation of C18-epoxides by CYP4F3B were in the same range, but at least 70-fold higher than that of CYP4F3A. Comparison of the apparent V_{max}/K_m ratios for the ω-hydroxylation of *Z*9(10)-EpOME and *Z*12(13)-EpOME by CYP4F isoforms highlighted their apparent catalytic efficiency and allowed us to rank them as follows: CYP4F3A > CYP4F3B > CYP4F2 for the ω-hydroxylation of C18-epoxides. Interestingly, both CYP4F3A and CYP4F3B catalyzed the ω-hydroxylation of the corresponding vicinal diol [9,10- and 12,13-dihydroxyC18:1 acid (DiOME)] generated by microsomes from insect cells to the corresponding trihydroxylated metabolites, in contrast to other recombinant enzymes such as CYP4F2 (Tables III, IV; see supplemental data). Furthermore, in additional experiments carried out to investigate the possible involvement of other human P450s in epoxide metabolism, we observed that in addition to CYP4F forms, three other P450 enzymes (i.e., CYP4A11, CYP3A4, and CYP2C8) also catalyzed *Z*9(10)-EpOME ω-hydroxylation at substantial rates. CYP4A11 proved to be a potent *Z*9(10)-EpOME ω-hydroxylase, with a turnover rate of 1.2 nmol of 18,9(10)-hydroxyepoxyoctadecenoic acid [18,9(10)-HEpOME] formed per minute per nanomole of P450. On the other hand, it catalyzed the hydroxylation reaction at much lower rates than CYP4F3A (12.3 nmol/min/nmol P450), CYP4F3B (8.6 nmol/min/nmol P450), and CYP4F2 (3.1 nmol/min/nmol P450). *Z*12(13)-EpOME was also ω-hydroxylated by CYP4A11, but at a much slower rate (0.3 nmol/min/nmol P450) than *Z*9(10)-EpOME. CYP2C8 and CYP2C9 both catalyzed mainly the (ω-1)-hydroxylation of *Z*9(10)-EpOME, but the rate was low compared with those of other recombinant P450s, although ω-hydroxylation was the major reaction of CYP2C9 with *Z*12(13)-EpOME as substrate. The turnover rate of the reactions [0.5 min^{-1} for ω-hydroxylation and 0.36 min^{-1} for (ω-1)-hydroxylation) remained ~16- and 5-fold lower than the rates by CYP4F3A and CYP4F3B, respectively. CYP2E1 seems not to be involved in the hydroxylation of C18-epoxides because no reaction product was detected after the incubation of substrates. CYP4A11, CYP4F3A, and CYP4F2 exhibited complete regiospecificity toward *Z*9(10)-EpOME and *Z*12(13)-EpOME, catalyzing only the ω-hydroxylation of leukotoxins.

EET and AA metabolism

We carried out additional experiments to study the metabolism of EETs by human liver microsomes and the involvement of recombinant CYP4F in oxidation reactions. In the absence of radiolabeled EETs, incubations were performed with unlabeled substrates. Metabolites were resolved and quantified by LC-MS ($APCI^-$). A representative profile of LC-MS analysis of metabolites generated from EETs by human microsomes is given in the supplemental data (Fig. VI). Enzyme activities were deduced from the peak areas of metabolites by assuming that ions had been generated with a similar intensity for the substrate and metabolites (see Materials and Methods). The chemical structures of the metabolites were confirmed by GC-MS analysis of Me/TMS derivatives. Table II (see supplemental data) lists the characteristic ions issued from the mass fragmentation of oxidized derivatives of EETs, and **Fig. 5** presents the $APCI^-$ mass spectra of ω-hydroxylated derivatives obtained from incubation with a series of EETs. The $APCI^-$ mass spectra of other metabolites are given in the supplemental data (Figs. IV, V). The mass spectra of the four ω-hydroxylated EETs all displayed signals at *m/z* 335 (M-H) and *m/z* 317 (M-H_2O) as well as a low-intensity signal at *m/z* 291 corresponding to the loss of CO_2 (M-44). Other specific ions, which resulted from α-cleavage at both sides of the epoxide group, the cleavage of the carbon chain at the epoxide ring [20,5(6)-HEET, *m/z* 128, 220; 20,8(9)-HEET, *m/z* 155, 167, 179; 20,11(12)-

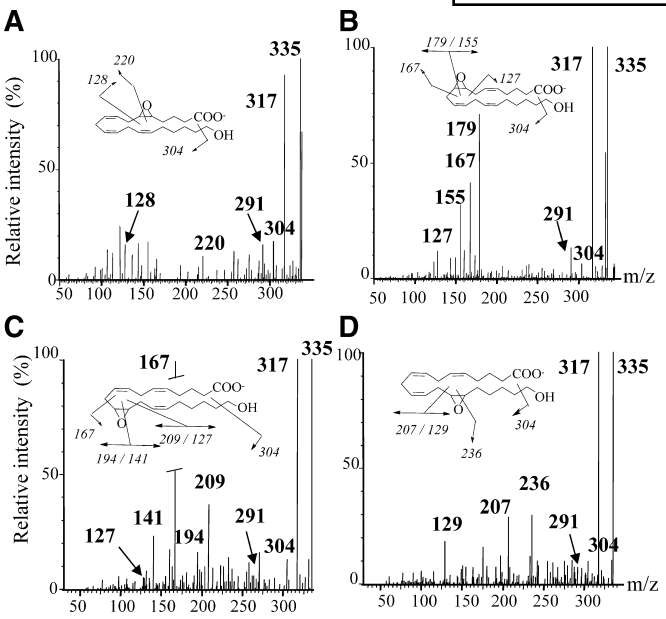

Fig. 5. Mass spectra of the 20-hydroxyepoxyeicosatrienoic acids (HEETs) generated by human liver microsomes. A: 20,5(6)-HEET; B: 20,8(9)-HEET; C: 20,11(12)-HEET; D: 20,14(15)-HEET. These four isomeric EETs (75 μM) were incubated with 0.3 mg of human liver microsomes and 1 mM NADPH at 37°C for 10 min and analyzed by RP-HPLC and mass spectrometric detection as described in Materials and Methods. The epoxide function is characterized by three fragmentations that generate informative signals. The position of the hydroxy function was characterized by a signal at *m/z* 304 [−31, loss of (OH)-CH_2^-] noted for the four positional enantiomers and informative signals corresponding to the α-cleavage between carbons of the oxirane.

TABLE 6. Metabolism of EETs by CYP4F isoforms and human liver microsomes (subject BR065)

Isoform	EET	Enzyme Activities		
		TriHET	20-HEET	DHET
		nmol/min/nmol P450		*nmol/min/mg protein*
CYP4F3B	5(6)-EET	0.22	0.57	0.033
	8(9)-EET	0.01	12.4	0
	11(12)-EET	0.02	0.44	0
	14(15)-EET	0.01	2.24	0.040
CYP4F3A	5(6)-EET	0.16	0.64	0.10
	8(9)- EET	0.05	14.1	0.43
	11(12)-EET	0.04	3.8	0.016
	14(15)-EET	0.27	9.2	0.12
CYP4F2	5(6)-EET	0.005	0.02	0.30
	8(9)- EET	0	1.0	0.055
	11(12)-EET	0	0.59	0.022
	14(15)-EET	0	0.61	0.20
		nmol/min/mg protein		
Human liver (BR065)	5(6)-EET	0.51	0.008	0.94
	8(9)-EET	0.57	0.46	4.0
	11(12)-EET	0.06	1.4	0.84
	14(15)-EET	0.14	0.2	10.8

Epoxyeicosatrienoic acids (EETs; 75 μM) were incubated with human recombinant CYP4F and 0.3 mg (0.68 nmol of P450 per milligram of protein) of microsomal protein and 1 mM NADPH at 37°C. Values shown are averages of triplicate determinations that differ for less than 10% of the means. The metabolites 20-hydroxyepoxyeicosatrienoic acid (20-HEET), dihydroxyeicosatrienoic acid (DHET), and a mixture of ω- and (ω-1)-trihydroxyeicosatrienoic acid (TriHET) were resolved and quantified by RP-HPLC with mass spectrometric detection as described in Materials and Methods.

HEET, *m/z* 127, 141, 167, 194, 209; and 20,14(15)-HEET, *m/z* 129, 207, 236), and the loss of $[HO\text{-}CH_2]^-$ (*m/z* 304, M-31) were in agreement with the structures of 20-hydroxylated EETs. The $APCI^-$ mass spectra (Fig. V; see supplemental data) of DHET resulting from the hydrolysis of epoxide by EH-like were very similar to those already described (42) and were mainly characterized by α-cleavage between the two carbons of the vicinal diol 5,6-DHET (*m/z* 115, 221), 8,9-DHET [*m/z* 155 (156-H), 179], 11,12-DHET [*m/z* 195 (196-H)], and 14,15-DHET (*m/z* 101). Trihydroxyeicosatrienoic acid (TriHET) were also detected by LC-MS analysis [*m/z* 353 $(M\text{-}H)^-$], but as a single peak (Fig. VI, see supplemental data). Thus, the rate of NADPH-dependent formation of TriHET corresponded to at least the sum of ω- and (ω-1)-hydroxylated DHETs (**Table 6**). EETs (75 μM) were incubated with liver microsomes (BR065) and recombinant CYP4F with and without NADPH. In the absence of the electron donor, the vicinal diols were mainly generated by human microsomes. Inhibition of EH-like from insect and liver microsomes with 100–200 μM cyclohexane oxide and elaidamide was unsuccessful, although these compounds inhibited the EH from rat (43). A high level of vicinal diol formation was measured in liver for *Z*14(15)-EET and *Z*8(9)-EET. In the microsomes from the BR065 subject, hydrolysis of *Z*14(15)-EET was clearly favored compared with that of *Z*8(9)-, *Z*5(6)-, and *Z*11(12)-EETs, in agreement with previously reported data (42). As for the oxidation of the vicinal diol generated by the microsomal EH-like, the best substrate was 8,9-DHET; it produced TriHET at a rate of 0.57 nmol/min/mg protein, whereas 14,15-DHET and 11,12-DHET were converted to TriHET at lower rates of 0.14 and 0.06 nmol/min/mg protein, respectively. Thus, more EETs were channeled into TriHETs when the conversion to DHETs was high, although the conversion of 14,15-DHET to TriHET was reduced compared with that of 8,9-DHET. In the presence of NADPH, *Z*5(6)-EET was rapidly converted by liver microsomes to a complex mixture of polar metabolites that were not completely separated by RP-HPLC. In addition, more than 90% of *Z*5(6)-EET were converted to many metabolites, although the residual substrate in the incubation mixture was ∼30% for the other three EETs (data not shown). Thus, the low rate observed for the conversion of *Z*5(6)-EET to 20,5(6)-HEET (0.01 nmol/min/mg protein) by liver microsomes presumably results from the lack of stability of this EET in the incubation medium, which drastically reduces its availability as a substrate. Table 6 shows that liver microsomes displayed extensive 20-hydroxylase activity in the presence of *Z*11(12)-EET (1.4 nmol/min/mg protein, 2.1 nmol/min/nmol total P450), whereas incubation with *Z*8(9)-EET and *Z*14(15)-EET led to the accumulation of 20-hydroxylated metabolites at lower rates (0.46 and 0.2 nmol/min/mg protein, respectively). Concerning EET

metabolism by recombinant CYP4F isoforms, Z8(9)-EET was the best substrate for the three isoforms CYP4F3A, CYP4F3B, and CYP4F2 and led mainly to 20,8(9)-HEET at turnover rates of 14.1, 12.4, and 1.0 min^{-1}, respectively. CYP4F2 exhibited restricted substrate specificity: it oxidized EETs, but not DHETs, in contrast to CYP4F3A and CYP4F3B.

We next examined the identity of the recombinant cytochrome P450 that generates 20-HETE in humans, because conflicting results have been reported on the capability of recombinant P450s to carry out AA hydroxylation (44, 45). The predominant catalyst of AA ω-hydroxylation in human tissues was initially identified as CYP4F2 (46, 47). More recently, Christmas et al. (33) demonstrated that CYP4F3B and CYP4F3A generate 20-HETE as their major metabolite. Incubations of 75 μM AA with recombinant CYP4F were performed to estimate the relative rate of metabolite formation in the presence of NADPH. With CYP4F3B, 20-HETE and 19-HETE were both generated at rates of 4.4 and 0.77 nmol/min/nmol P450, respectively. CYP4F3A catalyzed at lower rates: 2.95 and 0.19 nmol/min/nmol P450. As for CYP4F2, only 20-HETE was detected, being formed at a rate of 1.46 nmol/min/nmol P450, in agreement with previous experimental data by Powell et al. (47). Recombinant CYP4F3B converted AA into ω- and (ω-1)-hydroxylated metabolites with a ω-/(ω-1) ratio of 6:1; the ratio for CYP4F3A was ~15:1. These results are consistent with observations reported by others and confirm that the CYP4Fs are potent catalysts of AA ω-hydroxylation.

DISCUSSION

Here, we present direct evidence for the involvement of at least four cytochrome P450 isoforms, CYP4F2, CYP4F3A, CYP4F3B, and CYP4A11, in the ω-hydroxylation of C18-epoxides and EETs, whereas CYP4Fs were capable of catalyzing the hydroxylation of the vicinal diol derived from the hydrolysis of the oxirane ring by an EH-like enzyme. Our results clearly show that fatty acid epoxides and the corresponding vicinal diol are mainly hydroxylated at the terminal carbon position (ω) in human liver (n = 16). The subfamily CYP4F, known to inactivate the proinflammatory leukotriene LTB4, was found to convert fatty acid epoxides to ω-hydroxylated derivatives with an apparent K_m on the same order of magnitude as that measured for LTB4. Furthermore, we demonstrate for the first time that the P450 isoform mainly located in the liver (CYP4F3B) as well as that isolated from leukocytes (CYP4F3A) were the principal enzymes involved in these reactions. This finding does not exclude the possibility that other P450 enzymes, such as CYP4F8, CYP4F11, and CYP4F12, may also exhibit such activity.

These results demonstrate that another pathway besides conversion to vicinal diol exists for fatty acid epoxide inactivation. Human liver microsomes from 16 different subjects converted Z9(10)-epoxystearic acid to 18-hydroxy-9(10)-epoxystearic acid at rates (0.96 nmol/min/mg protein as a mean) ~4-fold higher than those measured from 10 subjects for LTB4 (0.25 nmol/min/mg protein as a mean) by Jin et al. (40) and 2-fold higher than for the vicinal diol production (0.5 nmol/min/mg protein as a mean). This represents the first characterization of an enzymatic pathway for leukotoxin biotransformation in human tissues. We also report that the EETs are excellent substrates for the human CYP4F isoforms and that they are rapidly oxidized to the corresponding 20-hydroxylated EETs, which were shown previously to bind with high affinity to the PPAR class of nuclear receptors (22). It appears that the CYP4F family plays a similar functional role as the CYP4A family in rat.

We also provide evidence for the involvement of the recombinant P450 CYP4A11 in the ω-hydroxylation of LTB4. In addition, our results show that recombinant CYP4A11 did not catalyze the hydroxylation of AA at a detectable level, in accordance with reports by Kikuta et al. (30). Moreover, CYP4A11 seems not to play a major role in the microsomal hydroxylation of C18-epoxides. This is supported by the lack of inhibition by lauric acid, a substrate of CYP4A11, and the complete competitive inhibition by LTB4, known as an endogenous substrate of CYP4F2 and CYP4F3. More controversial is the participation of CYP4A11 in the ω-hydroxylation of both AA and LTB4. Indeed, CYP4A11 was reported to catalyze the ω-hydroxylation of AA, but negligible activity was measured for the ω-hydroxylation of LTB4 (47). These results conflict with ours, which show both that CYP4A11 oxidizes this proinflammatory mediator at the terminal carbon position and also that CYP4A11 is unable to generate 20-HETE from AA at a detectable level. The complete inhibition of Z9(10)-EpSTA hydroxylation by LTB4 in human liver microsomes is in agreement with the involvement of CYP4A11 in LTB4 oxidation. The reasons for these discrepancies are unexplained, although heterologously expressed P450 enzymes are known to differ in their expression levels and activities, depending on the isoforms.

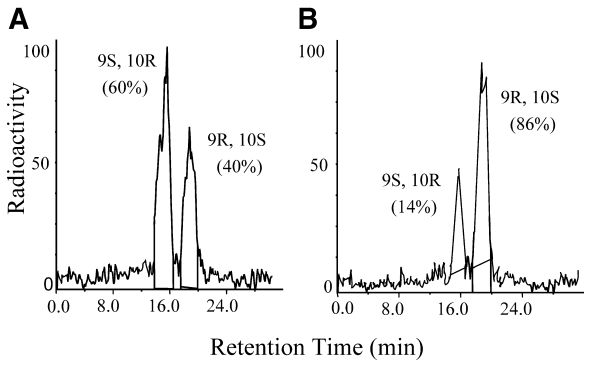

Fig. 6. Chiral-phase HPLC of radiolabeled 18,9(10)-HEpSTA generated by human recombinant CYP4F2 (A) and CYP4A11 (B). Metabolites were collected from the RP-HPLC column, converted to methyl ester, and analyzed using chiral-phase HPLC as described in Materials and Methods. Stereoisomers of 18,9(10)-HEpSTA were generated by CYP4F2 (A) and CYP4A11 (B).

Furthermore, chiral analysis clearly showed an enantiomeric excess in favor of the 9*S*,10*R* form of 18,9(10)-HEpSTA in the liver, whereas CYP4A11 generated mainly the 9*R*,10*S* enantiomer (**Fig. 6**). To tentatively determine which CYP4F isoform from liver was the major catalyst of C18-epoxides, we incubated *Z*9(10)-EpSTA with human microsomes in the presence of increasing concentrations of tocopherol. A recent report by Sontag and Parker (32) demonstrated that CYP4F2 was the unique P450 catalyzing the ω-hydroxylation of α- and γ-tocopherol. Surprisingly, α- and γ-tocopherol (50 μM) did not inhibit the hydroxylation of *Z*9(10)-EpSTA in liver microsomes either from rat (data not shown) or from eight human subjects, although incubations of CYP4F2 with tocopherol led to ω-hydroxylated derivatives (data not shown), in accordance to Sontag and Parker (32). These results suggest that in human liver the major P450 isoform involved in the ω-oxidation of C18-epoxides is CYP4F3B rather than CYP4F2.

The preponderance of a CYP4F3B isoform in liver would explain the monophasic Michaelis-Menten kinetics (data not shown) obtained for the hydroxylation of C18-epoxides, although we showed that at least three liver P450 isoforms exhibit appreciable ω-hydroxylase activity. Indeed, CYP4F3B has been reported to be the major CYP4F enzyme in liver (41), and enzyme kinetic analysis for the three recombinant CYP4F isoforms were monophasic in this study. The apparent K_m and V_{max} values obtained for the ω-hydroxylation of C18-epoxides (apparent K_m value ranging from 27.6 to 175 μM and apparent V_{max} ranging from 3.7 to 1.2 nmol/min/nmol total P450) in liver microsomes were on the same order of magnitude as those demonstrated for the ω-hydroxylation of LTB4 (K_m of 74.8 μM and V_{max} of 2.42 nmol/min/nmol P450) by human liver microsomes (40). Interestingly, the most efficient CYP4F for the ω-hydroxylation of C18-epoxides was CYP4F3A, showing apparent V_{max}/K_m values ranging from 1.7 to 0.05 (Table 4) and apparent K_m values of 6.3, 46.6, and 61.8 μM for *Z*9(10)-EpSTA, *Z*9(10)-EpOME, and *Z*12(13)-EpOME, respectively. The differences in efficiency exhibited by CYP4F3A and CYP4F3B for C18-epoxide hydroxylation were not comparable to that reported for LTB4 hydroxylation. Indeed, the apparent V_{max}/K_m values for LTB4 ω-hydroxylation were 44-fold higher for CYP4F3A than for CYP4F3B (40), although only a 4.6-fold difference was observed between the two isoforms for the ω-hydroxylation of *Z*9(10)-EpSTA.

On the other hand, CYP450 metabolites such as EETs and 20-HETE also act as second messengers for many biological processes, including cellular proliferation, apoptosis, inflammation, and homeostasis. Fewer data are available concerning the role of oxidized fatty acid from the C18 family in mammals. In addition to their role in the inflammation process as chemioattractant compounds, large amounts of dihydroxystearic and dihydroxyoleic acids as well as uncharacterized trihydroxyoctadecanoic and trihydroxyoctadecenoic acids have been measured in urine extracts from children with generalized peroxisomal disorders (46). From a phylogenic point of view, it is interesting that the metabolic pathway of C18-epoxides resembles that already described in higher plants (39). Interestingly, it has been shown that certain cutin monomers (i.e., 9,10,18-TriSTA), which are released from the plant cuticle by fungal cutinases, may protect the plant against fungal infection by inducing the plant defense mechanisms (2). It will be of great interest to further examine the possible metabolic and functional effects of these metabolites in mammals at the molecular and physiological levels.

Our results fill a gap in our understanding of the mechanisms mediating inactivation of toxic and proinflammatory endogenous compounds. CYP4F2 and CYP4F3, because of their abilities to metabolize both leukotoxins and LTB4, may play important roles in modulating the inflammatory cell response. Their reaction generates different octanoid products that may have potent, but yet unknown, biological effects. It is still not clear whether the ω-hydroxylation of fatty acid epoxides such as leukotoxins is an additional pathway for their biological inactivation or a means of producing biologically active compounds, but the recent work of Cowart et al. (22), showing the capability of the ω-hydroxy products derived from AA epoxide to bind to PPARα in vitro, is consistent with these molecules being biologically active.

In summary, this study has provided further evidence that P450s play a pivotal role in the generation of endogenous, biologically active compounds by revealing that the CYP4F gene family (at least CYP4F2, CYP4F3A, and CYP4F3B) are the major enzymes in human liver and leukocytes that convert the regioisomer EET to potent PPARα ligands, as already demonstrated in rodents (22). These enzymes also convert chemioattractant leukotoxins to more polar compounds with unknown physiological functions. Our results show the capability of microsomes from human liver to produce epoxy-hydroxy and trihydroxy fatty acid derivatives. The formation of this novel class of endogenous polyoxidized fatty acid is interesting in the light of the catalytic potential of CYP4F isoforms that are already known to inactivate not only the potent proinflammatory mediator LTB4 but also prostaglandins and lipoxins. The catalytic properties of CYP4F revealed here should provide a firm basis for forthcoming studies of the possible metabolic and functional effects of these metabolites in mammals. Further investigation of the induction and regulation of CYP4F in normal metabolism and human diseases possibly involving the nuclear receptor PPAR will be useful in extending our knowledge of their physiological roles.

V.L.Q. was supported by a fellowship from the Ministère de l'Education National, de la Recherche, et de la Technologie. This study was conducted under the Programme de Recherche d'Intérêt Régional funded by the Conseil Régional de Bretagne (PRIR-AOC429). Excellent technical assistance by Yvonne Dréano and Delphine Douguet is gratefully acknowledged. The authors also thank Jean-Pierre Noel and Olivier Moreau from the Commissariat à l'Energie Atomique for the synthesis of radiolabeled epoxides and Christophe Morisseau (University of California, Davis) for the gift of EH inhibitors.

REFERENCES

1. Moran, J. H., L. A. Mitchell, J. A. Bradbury, W. Qu, D. C. Zeldin, R. G. Schnellmann, and D. F. Grant. 2000. Analysis of the cytotoxic properties of linoleic acid metabolites produced by renal and hepatic P450s. *Toxicol. Appl. Pharmacol.* **168:** 268–279.
2. Kato, T., Y. Yamaguchi, T. Hirano, T. Yokoyama, T. Uyehara, T. Namaï, S. Yamanaka, and N. Harada. 1984. Unsaturated hydroxy fatty acids, the self defensive substances in rice plant against rice blast disease. *Chem. Lett.* **26:** 409–412.
3. Schweizer, P., A. Jeanguenat, D. Whitacre, J. P. Métraux, and E. Mösinger. 1996. Induction of resistance in barley against Erysiphe graminis f.sp. hordei by free cutin monomers. *Physiol. Mol. Plant Pathol.* **49:** 103–120.
4. Mumby, S. M., and B. D. Hammock. 1979. A partition assay for epoxide hydrases acting on insect juvenile hormone and an epoxide-containing juvenoid. *Anal. Biochem.* **92:** 16–21.
5. Jansen, M., A. J. Baars, and D. D. Breimer. 1986. Microsomal and cytosolic epoxide hydrolase in Drosophila melanogaster. *Biochem. Pharmacol.* **35:** 2229–2232.
6. Zheng, J., C. G. Plopper, J. Lakritz, D. H. Storms, and B. D. Hammock. 2001. Leukotoxin-diol: a putative toxic mediator involved in acute respiratory distress syndrome. *Am. J. Respir. Cell Mol. Biol.* **25:** 434–438.
7. Chu, I., D. C. Villeneuve, E. R. Nestmann, G. Douglas, G. C. Becking, R. Lough, and T. I. Matula. 1980. Subacute toxicity and mutagenicity of cis-9,10-epoxystearic acid. *Bull. Environ. Contam. Toxicol.* **25:** 400–403.
8. Greene, J. F., K. C. Williamson, J. W. Newman, C. Morisseau, and B. D. Hammock. 2000. Metabolism of monoepoxides of methyl linoleate: bioactivation and detoxification. *Arch. Biochem. Biophys.* **376:** 420–432.
9. Fauth, M., P. Schweizer, A. Buchala, C. Markstadter, M. Riederer, T. Kato, and H. Kauss. 1998. Cutin monomers and surface wax constituents elicit H_2O_2 in conditioned cucumber hypocotyl segments and enhance the activity of other H_2O_2 elicitors. *Plant Physiol.* **117:** 1373–1380.
10. Fang, X., T. L. Kaduce, N. L. Weintraub, S. Harmon, L. M. Teesch, C. Morisseau, D. A. Thompson, B. D. Hammock, and A. A. Spector. 2001. Pathways of epoxyeicosatrienoic acid metabolism in endothelial cells. Implications for the vascular effects of soluble epoxide hydrolase inhibition. *J. Biol. Chem.* **276:** 14867–14874.
11. Laethem, R. M., M. Balazy, and D. R. Koop. 1996. Epoxidation of C18 unsaturated fatty acids by cytochromes P4502C2 and P4502CAA. *Drug Metab. Dispos.* **24:** 664–668.
12. Draper, A. J., and B. D. Hammock. 2000. Identification of CYP2C9 as a human liver microsomal linoleic acid epoxygenase. *Arch. Biochem. Biophys.* **376:** 199–205.
13. Fahlstadius, P. 1988. Cis-9,10-epoxystearic acid in human leukocytes: isolation and quantitative determination. *Lipids.* **23:** 1015–1018.
14. Capdevila, J. H., P. Mosset, P. Yadagiri, S. Lumin, and J. R. Falck. 1988. NADPH-dependent microsomal metabolism of 14,15-epoxyeicosatrienoic acid to diepoxides and epoxyalcohols. *Arch. Biochem. Biophys.* **261:** 122–133.
15. Sevanian, A., R. A. Stein, and J. F. Mead. 1981. Metabolism of epoxidized phosphatidylcholine by phospholipase A2 and epoxide hydrolase. *Lipids.* **16:** 781–789.
16. Ozawa, T., M. Hayakawa, K. Kosaka, S. Sugiyama, T. Ogawa, K. Yokoo, H. Aoyama, and Y. Izawa. 1991. Leukotoxin, 9,10-epoxy-12-octadecenoate, as a burn toxin causing adult respiratory distress syndrome. *Adv. Prostaglandin Thromboxane Leukot. Res.* **21B:** 569–572.
17. Kolattukudy, P. E., T. J. Walton, and R. P. Kushwaha. 1973. Biosynthesis of the C18 family of cutin acids: omega-hydroxyoleic acid, omega-hydroxy-9,10-epoxystearic acid, 9,10,18-trihydroxystearic acid, and their delta12-unsaturated analogs. *Biochemistry.* **12:** 4488–4498.
18. Totani, Y., Y. Saito, T. Ishizaki, F. Sasaki, S. Ameshima, and I. Miyamori. 2000. Leukotoxin and its diol induce neutrophil chemotaxis through signal transduction different from that of fMLP. *Eur. Respir. J.* **15:** 75–79.
19. Dudda, A., G. Spiteller, and F. Kobelt. 1996. Lipid oxidation products in ischemic porcine heart tissue. *Chem. Phys. Lipids.* **82:** 39–51.
20. Zeldin, D. C., C. R. Moomaw, N. Jesse, K. B. Tomer, J. Beetham, B. D. Hammock, and S. Wu. 1996. Biochemical characterization of the human liver cytochrome P450 arachidonic acid epoxygenase pathway. *Arch. Biochem. Biophys.* **330:** 87–96.
21. Daikh, B. E., J. M. Lasker, J. L. Raucy, and D. R. Koop. 1994. Regio- and stereoselective epoxidation of arachidonic acid by human cytochromes P450 2C8 and 2C9. *J. Pharmacol. Exp. Ther.* **271:** 1427–1433.
22. Cowart, L. A., S. Wei, M. H. Hsu, E. F. Johnson, M. U. Krishna, J. R. Falck, and J. H. Capdevila. 2002. The CYP4A isoforms hydroxylate epoxyeicosatrienoic acids to form high affinity peroxisome proliferator-activated receptor ligands. *J. Biol. Chem.* **277:** 35105–35112.
23. Li, P. L., D. X. Zhang, Z. D. Ge, and W. B. Campbell. 2002. Role of ADP-ribose in 11,12-EET-induced activation of K(Ca) channels in coronary arterial smooth muscle cells. *Am. J. Physiol. Heart Circ. Physiol.* **282:** H1229–H1236.
24. Kozak, W., M. J. Kluger, A. Kozak, M. Wachulec, and K. Dokladny. 2000. Role of cytochrome P-450 in endogenous antipyresis. *Am. J. Physiol. Regul. Integr. Comp. Physiol.* **279:** R455–R460.
25. Campbell, W. B., J. R. Falck, and K. Gauthier. 2001. Role of epoxyeicosatrienoic acids as endothelium-derived hyperpolarizing factor in bovine coronary arteries. *Med. Sci. Monit.* **7:** 578–584.
26. Kroetz, D. L., and D. C. Zeldin. 2002. Cytochrome P450 pathways of arachidonic acid metabolism. *Curr. Opin. Lipidol.* **13:** 273–283.
27. French, S. W., M. Morimoto, R. C. Reitz, D. Koop, B. Klopfenstein, K. Estes, P. Clot, M. Ingelman-Sundberg, and E. Albano. 1997. Lipid peroxidation, CYP2E1 and arachidonic acid metabolism in alcoholic liver disease in rats. *J. Nutr.* **127 (Suppl.):** 907–911.
28. Miyazono, M., D. Zhu, R. Nemenoff, E. R. Jacobs, and E. P. Carter. 2003. Increased epoxyeicosatrienoic acid formation in the rat kidney during liver cirrhosis. *J. Am. Soc. Nephrol.* **14:** 1766–1775.
29. Holla, V. R., F. Adas, J. D. Imig, X. Zhao, E. Price, Jr., N. Olsen, W. J. Kovacs, M. A. Magnuson, D. S. Keeney, M. D. Breyer, J. R. Falck, M. R. Waterman, and J. H. Capdevila. 2001. Alterations in the regulation of androgen-sensitive Cyp 4a monooxygenases cause hypertension. *Proc. Natl. Acad. Sci. USA.* **98:** 5211–5216.
30. Kikuta, Y., E. Kusunose, T. Kondo, S. Yamamoto, H. Kinoshita, and M. Kusunose. 1994. Cloning and expression of a novel form of leukotriene B4 omega-hydroxylase from human liver. *FEBS Lett.* **348:** 70–74.
31. Kikuta, Y., M. Kato, Y. Yamashita, Y. Miyauchi, K. Tanaka, N. Kamada, and M. Kusunose. 1998. Human leukotriene B4 omega-hydroxylase (CYP4F3) gene: molecular cloning and chromosomal localization. *DNA Cell Biol.* **17:** 221–230.
32. Sontag, T. J., and R. S. Parker. 2002. Cytochrome P450 omega-hydroxylase pathway of tocopherol catabolism. Novel mechanism of regulation of vitamin E status. *J. Biol. Chem.* **277:** 25290–25296.
33. Christmas, P., S. R. Ursino, J. W. Fox, and R. J. Soberman. 1999. Expression of the CYP4F3 gene. Tissue-specific splicing and alternative promoters generate high and low K(m) forms of leukotriene B(4) omega-hydroxylase. *J. Biol. Chem.* **274:** 21191–21199.
34. Zhang, X., and J. P. Hardwick. 2000. Regulation of CYP4F2 leukotriene B4 omega-hydroxylase by retinoic acids in HepG2 cells. *Biochem. Biophys. Res. Commun.* **279:** 864–871.
35. Kikuta, Y., E. Kusunose, and M. Kusunose. 2002. Prostaglandin and leukotriene omega-hydroxylases. *Prostaglandins Other Lipid Mediat.* **68–69:** 345–362.
36. Kikuta, Y., Y. Miyauchi, E. Kusunose, and M. Kusunose. 1999. Expression and molecular cloning of human liver leukotriene B4 omega-hydroxylase (CYP4F2) gene. *DNA Cell Biol.* **18:** 723–730.
37. Berthou, F., D. Ratanasavanh, C. Riche, D. Picart, T. Voirin, and A. Guillouzo. 1989. Comparison of caffeine metabolism by slices, microsomes and hepatocyte cultures from adult human liver. *Xenobiotica.* **19:** 401–417.
38. Omura, T., and R. Sato. 1964. The carbon monoxide-binding pigment of liver microsomes. I. Evidence for its hemoprotein nature. *J. Biol. Chem.* **239:** 2370–2378.
39. Pinot, F., J. P. Salaun, H. Bosch, A. Lesot, C. Mioskowski, and F. Durst. 1992. Omega-hydroxylation of Z9-octadecenoic, Z9,10-epoxystearic and 9,10-dihydroxystearic acids by microsomal cytochrome P450 systems from Vicia sativa. *Biochem. Biophys. Res. Commun.* **184:** 183–193.
40. Jin, R., D. R. Koop, J. L. Raucy, and J. M. Lasker. 1998. Role of human CYP4F2 in hepatic catabolism of the proinflammatory agent leukotriene B4. *Arch. Biochem. Biophys.* **359:** 89–98.
41. Christmas, P., J. P. Jones, C. J. Patten, D. A. Rock, Y. Zheng, S. M. Cheng, B. M. Weber, N. Carlesso, D. T. Scadden, A. E. Rettie, and

R. J. Soberman. 2001. Alternative splicing determines the function of CYP4F3 by switching substrate specificity. *J. Biol. Chem.* **276:** 38166–38172.

42. Zeldin, D. C., C. R. Moomaw, N. Jesse, K. B. Tomer, J. Beetham, B. D. Hammock, and S. Wu. 1996. Biochemical characterization of the human liver cytochrome P450 arachidonic acid epoxygenase pathway. *Arch. Biochem. Biophys.* **330:** 87–96.
43. Fang, X., N. L. Weintraub, C. L. Oltman, L. L. Stoll, T. L. Kaduce, S. Harmon, K. C. Dellsperger, C. Morisseau, B. D. Hammock, and A. A. Spector. 2002. Human coronary endothelial cells convert 14,15-EET to a biologically active chain-shortened epoxide. *Am. J. Physiol. Heart Circ. Physiol.* **283:** H2306–H2314.
44. Palmer, C. N., T. H. Richardson, K. J. Griffin, M. H. Hsu, A. S. Muerhoff, J. E. Clark, and E. F. Johnson. 1993. Characterization of a cDNA encoding a human kidney, cytochrome P-450 4A fatty acid omega-hydroxylase and the cognate enzyme expressed in Escherichia coli. *Biochim. Biophys. Acta.* **1172:** 161–166.
45. Hoch, U., J. R. Falck, and P. R. de Montellano. 2000. Molecular basis for the omega-regiospecificity of the CYP4A2 and CYP4A3 fatty acid hydroxylases. *J. Biol. Chem.* **275:** 26952–26958.
46. Street, J. M., J. E. Evans, and M. R. Natowicz. 1996. Glucuronic acid-conjugated dihydroxy fatty acids in the urine of patients with generalized peroxisomal disorders. *J. Biol. Chem.* **271:** 3507–3516.
47. Powell, P. K., I. Wolf, R. Jin, and J. M. Lasker. 1998. Metabolism of arachidonic acid to 20-hydroxy-5,8,11,14-eicosatetraenoic acid by P450 enzymes in human liver: involvement of CYP4F2 and CYP4A11. *J. Pharmacol. Exp. Ther.* **285:** 1327–1336.